

ORIGINAL RESEARCH PAPER

Thermo-Hydraulic Investigation of Nanofluid as a Coolant In VVER-440 Fuel Rod Bundle

S. Jalili Palandi^{1,2}, A. Rahimi-Sbo¹, R. Mohammadyari¹, M. Rahimi-Esbo^{1,2,*}

¹Department of Mathematics, Buinzahra Branch, Islamic Azad University, Buinzahra, I.R. Iran

²School of Mechanical Engineering, Babol University of Technology, Babol, I.R. Iran

ARTICLE INFO.

Article history

Received 19 July 2014

Accepted 15 May 2015

Keywords

Heat transfer coefficient

Nanofluid

Particle diameter

Rod bundle

Volume fraction

Abstract

The main purpose of this study is to perform numerical simulation of nanofluids as the coolant in VVER-440 fuel rod bundle. The fuel rod bundle contains 60 fuel rods with length of 960 mm and 4 spacer grids. In VVER-440 fuel rod bundle the coolant fluid (water) is in high pressure and temperature condition. In the present Thermo-hydraulic simulation, water-AL₂O₃ nanofluids containing various volume fractions of AL₂O₃ nanoparticles are investigated. Calculations performed for Reynolds number of 125000 to 203000, nanoparticles fraction of 0 to 0.05 and nanoparticles diameter of 20 to 100 nm. In this literature, the effects of diameter and volume fraction of nanoparticles on thermo-hydraulic parameters are studied. To perform correct calculation, different grid qualities of fuel rod bundle are studied and results are compared with reference results. Empirical studies show that as the temperature rises, the effect of nanoparticles on enhancing thermal conductivity intensifies. So it can be said that as the VVER-440 fuel rod bundle works in high temperature condition, using the nanofluids in this rod bundle can be effective. Results of our numerical study showed that by using nanofluids as coolant fluid the heat transfer coefficient increases significantly and heat transfer enhancement raises with increase in volume fraction of nanoparticle.

1. Introduction

Detailed knowledge of the thermo-hydraulic processes is very important in the case of fuel rod bundles of nuclear reactors from the design and safe operation viewpoint. In pressurized water reactor, control of coolant fluid temperature and pressure is important for the view of safety. For example, a spot with high temperature in fuel rods cladding can be

dangerous. Pressurized water reactors (PWR) are the most common nuclear reactors that use water as coolant fluid. In these reactors because of high water pressure, the boiling temperature is high and the fluid is always liquid, thus the reactors coolant fluid is known as a high pressure and temperature water. The VVER-440 reactor is the Russian version of the commercial PWR reactor that has a hexagonal fuel rod bundle.

Recently, many experimental and numerical studies on the flow field and heat transfer in fuel rods bundle have been done.

*Corresponding author

Email address: Rahimi.esbo@stu.nit.ac.ir

Nomenclature		T	Temperature (K)
$C_{\varepsilon 1} C_{\varepsilon 2} C_{\varepsilon 3}$	constants in the model transport equations	t	time (s)
C_p	specific heat ($\text{kJ}\cdot\text{kg}^{-1}\cdot\text{K}^{-1}$)	V_b	Brownian velocity of nanoparticles ($\text{m}\cdot\text{s}^{-1}$)
d_f	diameter of base fluid molecules (m)	Greek Symbols	
d_p	average diameter of nanoparticles (m)	α	thermal diffusivity ($\text{m}^2\cdot\text{s}^{-1}$)
F_1	blending functions in k- ω SST model	δ	center-to-center distance of nano particles(m)
h	height of rod bundle (mm)	ε	turbulent dissipation rate ($\text{m}^2\cdot\text{s}^{-3}$)
h_{ave}	heat transfer coefficient ($\text{W}\cdot\text{m}^{-2}\cdot\text{K}^{-1}$)	μ	dynamic viscosity ($\text{kg}\cdot\text{m}^{-1}\cdot\text{s}^{-1}$)
K_b	Boltzmann number ($=1.3807 \times 10^{-23} \text{ J}\cdot\text{K}^{-1}$)	ρ	density ($\text{kg}\cdot\text{m}^{-3}$)
k	turbulence kinetic energy ($\text{m}^2\cdot\text{s}^{-2}$)	ω	specific dissipation rate of turbulent kinetic energy (S^{-1})
L_f	free average distance of water molecules(m)	Subscripts	
N	parameter for adapting the results with experimental data	ave	average
pr	Prandtl number of nanofluid	f	Base fluid
q"	uniform heat flux ($\text{W}\cdot\text{m}^{-2}$)	nf	nanofluid
Re	Reynolds number	P	Particle
		w	wall

Conner et al. [1] presented a CFD methodology to model single-phase, steady-state conditions in PWR fuel assemblies and performed experiments to validate the CFD methodology for this fuel assemblies. Their numerical simulation results were compared to experimental results and concluded that the proposed CFD model is suitable for predict the fluid behavior in PWR fuel rod bundle.

Tóth et al. [2] numerically simulated a60 degrees reactor of VVER-440 fuel rod bundle includes 21 fuel rods and 4spacer grids.

Three turbulence models for the flow in fuel rod bundle channels were considered and temperature of fuel rods cladding, cooling fluid temperature, coolant fluid pressure, turbulent kinetic energy and heat transfer coefficient were investigated. The results suggested that by using k- Ω model, higher heat transfer coefficient was obtained other turbulence models.

Abdi et al. [3] investigated the role of long and short mixing vanes in VVER-440 fuel rod bundle with length of 240 and 960 mm to raise the heat transfer coefficient. Their results indicated that short length mixing vanes produce higher heat transfer coefficient than long length mixing vanes.

Rahimi et al. [4] performed a thermal-hydraulic analysis of coolant fluid in VVER-1000 reactor core using the porous media approach. To validate the

calculations, they compared their results with the results of COBRA EN code that showed good agreement. Their simulation showed that the axial pressure drop of the coolant that flows through the fuel-assemblies is caused by the coolant-wall friction and the abrupt geometry changes through a channel, especially on grid spacers.

Jabbari et al. [5] analyzed an in-operation VVER-1000 reactor thermal power by a thermal method for the primary circuit. The calculated values of reactor thermal power by the thermal method are compared with the reactor power measured by the instruments. Their investigation showed that the thermal method, which is used in the average power calculation, leads to a smaller error in comparison with the other applied methods.

Another way to increase the heat transfer in rod bundle is improving the thermal properties of coolant fluid.

Therefore, different techniques have been suggested to increase the heat transfer properties of fluids. Researchers have also tried to enhance the thermal conductivity of base fluids by suspending micro or larger-sized solid particles in fluids, since the thermal conductivity of solid is typically higher than that of liquids. However, due to the large size and high density of the particles, there is no proper technique to avoid the solid particles from settling out of

suspension. Thus, fluids with dispersed coarse-grained particles have not yet been commercialized.

Fluids with suspended nanoparticles is called nanofluid, a term proposed in 1995 by Choi [6] of the Argonne National Laboratory, USA. This new type of fluid is manufactured by dispersing a small amount of solid nanoparticles in conventional heat transfer fluids. Some advantages of nanofluids that make them useful are: high effective thermal conductivity, high stability, less clogging and abrasion. The much larger relative surface area of nanoparticles, compared to those of conventional particles, should not only significantly improve the heat transfer capabilities, but also should increase the stability of the suspensions. Also, nanofluids due to containing tiny particles can improve abrasion-related properties as compared to the conventional solid/fluid mixtures.

To explain the reasons for the anomalous raise of the thermal conductivity in nanofluid, Koblinski et al. [7] and Eastman et al. [8] proposed four possible mechanisms: Brownian motion of the nanoparticles, molecular-level layering of the liquid at the liquid/particle interface, the nature of heat transport in the nanoparticles, and the effects of nanoparticles clustering.

Ghaffari et al. [9] numerically studied turbulent mixed convection heat transfer of the Al_2O_3 -water nanofluid in a horizontal curved tube using two phase model approach. The results indicated that at the low Grashof number, the turbulent intensity raised with increasing nanoparticle volume fraction but at the higher Grashof number using higher nanoparticle concentration, decreased the flow turbulent intensity across the vertical plane.

Behzadmehr et al. [10] simulated turbulent forced convection of a nanofluid in a circular tube. Two phase mixture models were applied for calculations. The results indicated that adding 1% nanoparticles increased the Nusselt number by more than 15%. Their study showed that to improve accuracy of calculations, effective physical properties must be considered for nanofluid rather than volume weighted average of particles and fluid properties.

Abdellahoum et al. [11] numerically investigated turbulent forced convection of a nanofluid over a heated cavity in a horizontal duct. Numerical simulations are carried out for pure water and four different nanofluids (water-Cu, water-CuO, water-Ag and water- Al_2O_3) by ANSYS FLUENT 14.0 CFD code. They concluded that the average Nusselt number increases with volume fraction of nanoparticles for the whole tested range of Reynolds number.

Moghadassiet al. [12] presented a CFD modeling of a horizontal circular tube to investigate the effect of nanofluids on laminar forced convective heat transfer. The water-based Al_2O_3 and Al_2O_3 -Cu hybrid nanofluid with 0.1% volume concentration was considered. Their results showed a higher convective heat transfer coefficient for the hybrid nanofluid.

Cooling applications of nanofluid showed that nanofluid can be applied to power plant cooling and safety systems caused by their enhanced properties such as thermal conductivity. Several investigations about practical application of nanofluid in nuclear reactor technology have been performed. Buongiorno et al. [13] investigated feasibility of using nanofluids in light water reactors. The analysis indicated that nanofluid can raise the in-vessel retention capability of nuclear reactors as much as 40%.

Hadad et al. [14] investigated the effects of different types and volume fractions of nanoparticles with the Monte-Carlo method. They concluded that the small change of the multiplication factor can be reached by Al_2O_3 /water nanofluids, and maximum radial power peaking factors are invariant to different volume fractions of nanoparticle and stay in the statistical error of Monte-Carlo calculations.

Zarifi et al. [15] performed a thermal-hydraulic analysis of nanofluid as the coolant fluid in VVER-1000 reactor core using the porous media approach. They studied water-based nanofluids containing various volume fractions of Al_2O_3 and TiO_2 nanoparticles. The results showed that the temperature of the coolant fluid has been risen with the concentration of nanoparticles.

Hadad et al. [16] investigate the thermal hydraulic attributing nanofluid in a fuel assembly coolant channel of a VVER-1000 reactor using computational fluid dynamic, and heat transfer coefficient, pressure drop and temperature differences was calculated for water/ Al_2O_3 nanofluid.

In this study, water- Al_2O_3 nanofluid is considered as the cooling fluid and the effects of nanoparticles diameter and volume fraction on the heat transfer coefficient and pressure drop of fluid flow in VVER-440 rod bundle channels is studied.

2. Model description

Fuel assemblies of the VVER-440 type reactors consist of three main parts: assembly legs, rod bundles and assembly heads.

The simulated rod bundles include 61 fuel rods arranged in a triangular configuration, 4 spacer grids

and a central tube for the self-powered neutron detectors.

The height of fuel rod bundle is 960 mm. The pitch of fuel rods and spacer grids are 12.2 and 240 mm, respectively. As well as the outer diameter of the fuel rods is 9.1 mm. Figure 1 shows this rod bundle and for better visibility, the rod bundle is shown semi-transparent.

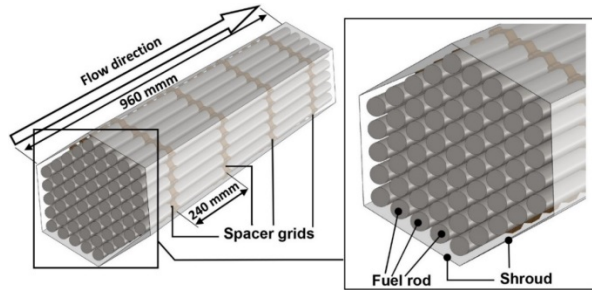


Fig. 1. Full model of studied fuel rod bundle

In each spacer grid, each rod is kept by three holder springs with hexagonal geometry. The constant distance between the fuel rods is maintained by spacer grids placed along the length of the rod bundle. The coolant media flows axially in the sub-channels formed between the rods. Figure 2 represents the spacer grids of the full model. The height of spacer grids, thickness of holder spring and thickness of other parts of spacer grids are 10, 0.25 and 0.5 mm, respectively.

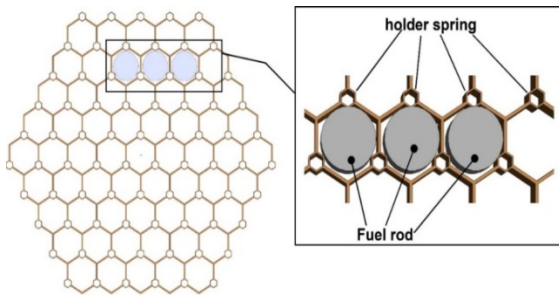


Fig. 2. Full model of studied spacer grids

Since the fuel rod bundle is hexagonal and the boundary conditions are symmetric, the size and time of numerical computation can be decreased by modeling a 60 degree segment of fuel rod bundle and the results would be closer to reality.

Figure 3 illustrates the 60 degree segment of fuel rod bundle. This geometry includes 12 fuel rods (8 full rods and 4 half rods), central tube, 4 spacer grids and walls of the shroud. Wall thickness of the shroud was ignored and the wall was modeled as a thin surface. This simplification is logical, since considering the

thickness of the shroud about 2 mm, the thermal conductivity of the shroud material is fairly high.

The spacer grids enhance the turbulence of the flow, therefore the heat transfer coefficient increases. Also, using the spacer grids increases the pressure drop due to blocking higher area of flow sub-channels.

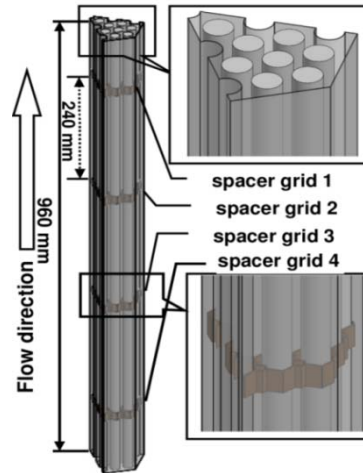


Fig. 3. 60 degree segment of studied fuel rod bundle

Figure 4 illustrates the 60 degree segment of spacer grid. In Figure 4 exact position of fuel rods and sub-channels in spacer grids are shown by putting a fuel rods.

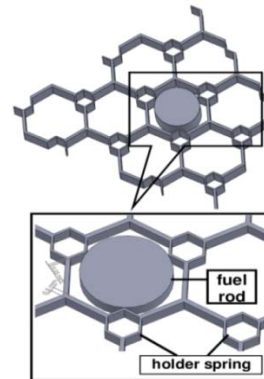


Fig. 4. 60 degree segment of spacer grid

3. Simulation and boundary conditions

Numerical investigation requires enough definition of the boundary conditions. In this effort, the coolant media is introduced to the domain with the velocity of 3.25 m/s and temperature of 540 K. The physic of the problem denotes the turbulence condition in which turbulence intensity is considered close to 3.5%. The hydraulic diameter of the bundle is 7.782 mm. The coolant media is assumed to be water in about 124 bar pressure. No slip adiabatic condition is considered for

the walls of the shroud, though for the walls of the rod, no slip boundary condition with constant heat flux about 1047340 W/m² is set. At the outlet of the rod bundle, the pressure was defined to be zero. With respect to the average value of the axial heat flux in modelling of the domain in the VVER-440 reactor at full power (1375 MW), the maximal core heat flux doesn't change sensibly from the average amount. Heat conduction in the spacer grids was ignored since the walls were thin (0.25–0.5mm) and the contact areas between them and fuel rods are rather small. All walls are considered to be smooth, and no roughness was determined for them. Symmetry boundary conditions are defined on symmetry planes. Figure 5 shows some boundary conditions schematically for a section of this fuel rod bundle.

In this paper turbulence is modelled with the k- ω SST model. In the k- ω SST model transport equations for the turbulence kinetic energy and turbulence dissipation are as following:

$$\frac{\partial(\rho k)}{\partial t} + \frac{\partial(\rho U_j k)}{\partial X_j} = \frac{\partial}{\partial X_j} \left[\left(\mu + \frac{\mu_t}{\sigma_k} \right) \frac{\partial k}{\partial X_j} \right] + P_k - \beta' \rho k \quad (1)$$

Blending function of F1 is used in the model which activates the model close to the wall and model in the outer region.

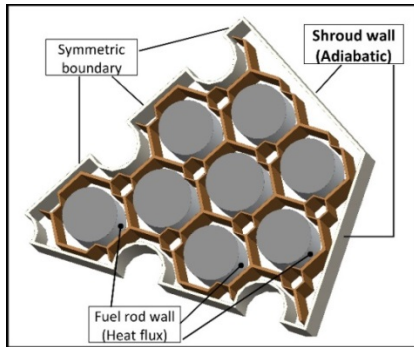


Fig. 5. Some boundary conditions

$$\frac{\partial}{\partial t}(\rho \omega) + \frac{\partial(\rho U_j \omega)}{\partial X_j} = \frac{\partial}{\partial X_j} \left[\left(\mu + \frac{\mu_t}{\sigma_\omega} \right) \frac{\partial \omega}{\partial X_j} \right] + \alpha \frac{\omega}{k} P_k - \beta \rho \omega + (1 - F_1) \frac{2\rho}{\sigma_{\omega 2}} \frac{\partial k}{\partial X_j} \frac{\partial \omega}{\partial X_j} \quad (2)$$

All equations are solved using control volume formulation through an open-source CFD package OpenFOAM [17]. The pressure field and velocity field are coupled together through the SIMPLE

method. Also, second order upwind method is used for the convective and diffusive terms.

In order to define a suitable mesh resolution for the rod bundle geometry, mesh sensitivity study should be performed. So, four mesh numbers were generated applying different mesh densities on the spacer grid parts while maintaining the remaining global mesh spacing unchanged.

Figures 6 and 7 illustrate average static pressure of coolant media and cladding average temperature at different mesh resolutions, respectively. Results indicated that there was little grid influence for grid numbers greater than 2,199,607 elements; therefore this grid number is used for this investigation.

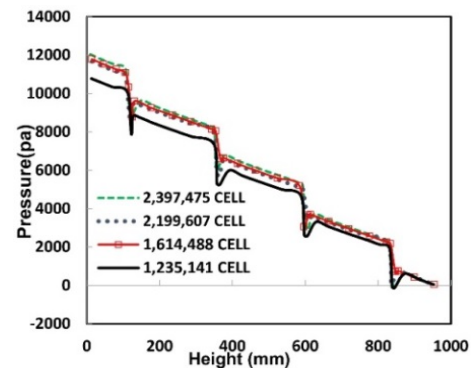


Fig. 6. Pressure of coolant fluid in the flow direction

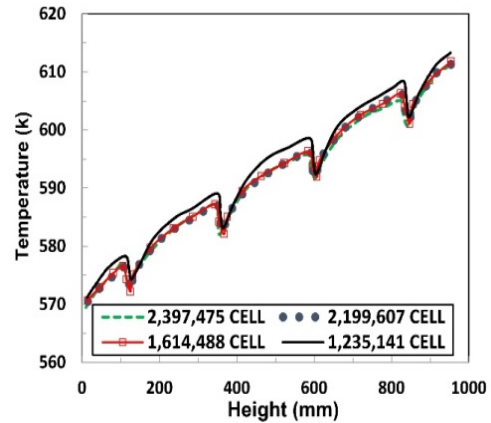


Fig. 7. The cladding temperature of fuel rod bundle

To meshing the nine sub-domains of fuel rod bundle, two mesh types is generated. Figure 8 illustrates some details of unstructured generated meshes for the simulation. Sub-domains 2, 4, 6 and 8 are mesh type I and consist of shell, fuel rods and spacer grids with length of 10 mm. Sub-domains 1, 3, 5, 7 and 9 are mesh type II and consist of shell and rods. The final meshes were defined with a global edge length of 0.8 mm. Near the walls, 4 layers of in flatted

elements with an expansion factor of 1.3 and first layer height of 0.025 mm are used. For mesh type I, containing the spacer grid, a superficial edge length of 0.3 mm was defined. Figure 9 shows the mesh on the outer surface of fuel rod bundle.

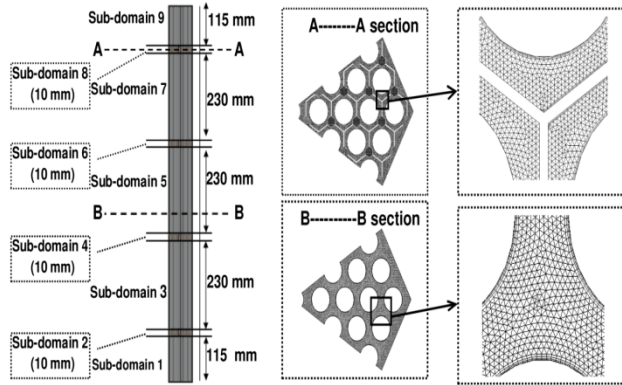


Fig. 8. Mesh cross section in (A-----A) and (B-----B) regions.

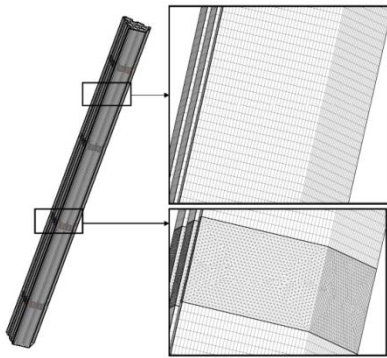


Fig. 9. Mesh on the outer surface of fuel rod bundle

4. Validation

To analyze the precision of the model assumptions and the numerical procedure, got results are compared to results of Abdi et al. [3]. In this step, the fluid inlet velocity is considered to be 3.25m/s. As shown in figures 10 and 11, the results are in good agreement with numerical results of Abdi et al. [3]. Because of no experimental data numerical results are used for validation of simulation.

In figure 10 it can be seen that the cladding average temperature decreases at the spacer grid. When the coolant flows into the holes of the spacer grid the velocity and the turbulence kinetic energy grow rapidly, therefore the conditions of heat transfer improve and the temperature of the cladding decreases suddenly. Behind the spacer grid, the temperature of the cladding rises again first, because the turbulence kinetic energy decays and the conditions of the heat

transfer become worse. Figure 11 shows four local pressure drops.

The explanation of this behaviour is that the coolant flow velocity increases in the spacer grids because of contraction and it causes a local pressure drop.

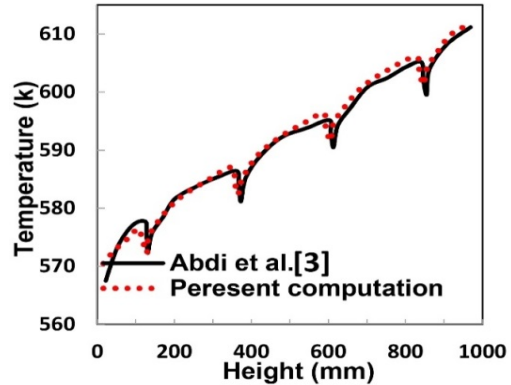


Fig. 10. The cladding temperature of fuel rod bundle

Behind the spacer grids the flow velocity cuts rapidly and the static pressure increases to a value which is less than it was in front of the spacer grids, because that spacer grids cause a separation loss.

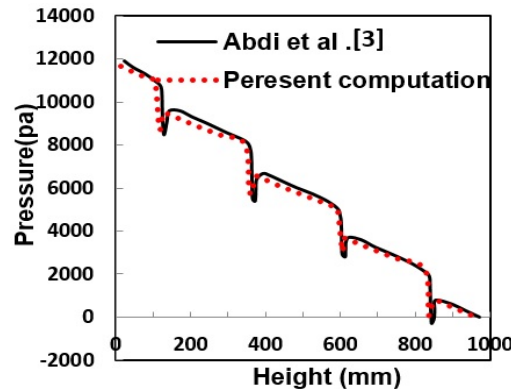


Fig. 11. Pressure of coolant fluid in the flow direction

Coolant fluid with specific temperature enters to rod bundle channels and in the flow direction its temperature increases with enhancing the height. Coolant fluid reaches to highest temperature at outlet (the highest height). Outlet temperature distributing the coolant fluid is presented in figure 12. It can be seen that the coolant temperature increases with enhancing the height.

5. The role of Nanofluids in heat transfer

To study the role of Nanofluids in heat transfer, many parameters should be considered. Nanofluids

thermal properties are about the temperature, mean nanoparticle diameter, nanoparticle volume fraction, nanoparticle density and the based fluid physical properties.

Janga et al. [18] showed that as the temperature rises, the effect of nanoparticles on enhancing thermal conductivity intensifies. So it can be said that as the VVER-440 fuel rod bundle works in high temperature condition, using the nanofluids in this rod bundle can be effective.

In this study water-AL₂O₃ nanofluid is considered as coolant fluid. The Nanofluid is assumed as a single phase and incompressible fluid. For the numerical calculations, thermal conductivity, viscosity, density and heat capacity of the Nanofluid is embedded to the open source code.

The thermal conductivity of the nanofluid is calculated from Chon et al. [19], which is expressed in the following form:

$$\frac{K_{nf}}{K_f} = 1 + 46.7\phi^{0.746} \left(\frac{d_f}{d_p}\right)^{0.369} \times \left(\frac{K_p}{K_f}\right)^{0.7476} Pr_f^{0.9955} Re_p^{1.2321} \quad (3)$$

$$Pr_f = \frac{\mu_f}{\rho_f \alpha_f} \quad (4)$$

$$Re_p = \frac{\rho_f K_b T}{3\pi\mu^2 L_f^2} \quad (5)$$

Where K_b is the Boltzmann constant, 1.3807×10^{-23} and L_f is the free average distance of water molecules that according to suggestion of Chon et al. [19] is taken as 0.17 nm.

Minister et al. [20] approved the accuracy of this model. The viscosity of the nanofluid is approximated as viscosity of the base fluid μ_f containing dilute suspension of fine spherical particles, as given by Masoumi et al. [21].

$$\frac{\mu_{nf}}{\mu_f} = 1 + \frac{\rho_p V_d d_p^2}{72N \delta} \quad (6)$$

$$V_b = \left(\frac{1}{d_p}\right) \sqrt{\frac{18K_b T}{\pi\rho_p d_p}} \quad (7)$$

$$N = (C_1 d_p + C_2)\phi + (C_3 d_p + C_4) \quad (8)$$

$$\delta = 3\sqrt{\frac{\pi}{6\phi}} \times d_p \quad (9)$$

N is a parameter for adapting the results with experimental data, where

$$C_1 = -1.133 \times 10^{-6}, C_2 = -2.771 \times 10^{-6}$$

$$C_3 = 9 \times 10^{-8}, C_4 = -3.93 \times 10^{-7}$$

The density and specific heat capacity of the nanofluids are calculated by using the Pak and Cho [22] correlations, which are defined as follows:

$$\rho_{nf} = \phi\rho_p + (1-\phi)\rho_f \quad (10)$$

$$Cp_{nf} = \frac{(1-\phi)\rho_f Cp_f + \phi\rho_p Cp_p}{\rho_{nf}} \quad (11)$$

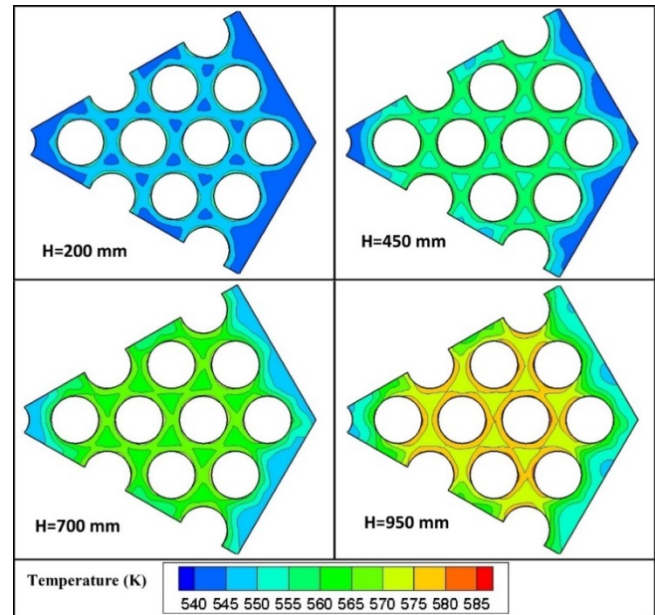


Fig. 12. Contours of coolant fluid temperature in different heights

Table 1 shows the thermo-physical properties of AL₂O₃ at temperature of 540K and water at pressure of 12.4 MPa and temperature of 540 K.

Table 1
Thermo-physical properties of Al_2O_3 and water.

Al_2O_3	3970	1000	22
water	746	5268	0.5786

In this study water- Al_2O_3 nanofluid is considered as coolant fluid and effects of volume fraction and diameter of nanoparticles on the heat transfer coefficient and pressure drop are investigated. Average heat transfer coefficient is one of the important parameters in VVER-440 rod bundle that can be calculated from equation 12.

$$h_{ave} = \frac{\dot{q}_w''}{T_w - T_{ave}} \quad (12)$$

T_w, T_{ave} are rod cladding temperature and average of coolant fluid temperature respectively and \dot{q}_w'' is heat flux of fuel rods ($1,047,340 \text{ W/m}^2$).

Figure 13 shows the changes of heat transfer coefficient at different volume fractions and different Reynolds numbers at nanoparticles diameter of 50nm. In table 2 total mean of heat transfer coefficient in rod bundle, at different Reynolds numbers is presented.

As it can be seen, the heat transfer coefficient rises with enhancement of the nanoparticle volume fraction for all Reynolds numbers. Results show that the addition of solid nanoparticles to the base fluid has led to a rise in mean heat transfer coefficient of fuel rod bundle. Equation 3 shows that, addition of nanoparticles increases the thermal conductivity of the base fluid. This enhancement in thermal conductivity increases the convective heat transfer coefficient. Also, chaotic movement of the solid particles in the flow will disturb the thermal boundary layer formation on the wall surface of fuel rod bundle (walls of rods and shell). As a result of this disturbance, the development of the thermal boundary layer is delayed. Because higher heat transfer coefficients are obtained at the inlet region of the rod bundle, the delay in thermal boundary layer formation resulted by adding nanoparticles will enhance the mean heat transfer coefficient. At higher volume fractions of nanofluids, the thermal conductivity of nanofluid and the disturbance effect of the solid nanoparticles will raise. So, nanofluids with higher volume fractions have higher convective heat transfer coefficients.

Pressure drop is an important factor in fuel rod bundle. The pressure drop and coolant pumping power are strongly related. Figure 14 shows total pressure drop in fuel rod bundle for nanoparticle diameter of 50nm at different volume fractions and different Reynolds numbers. It is clear that a linear relationship exists between the pressure drop and volume fraction of nanoparticles. This figure shows that enhancing nanoparticles volume fraction increases the pressure drop. According to equation 6 the viscosity of Nanofluids rises with increment of nanoparticles volume fraction. Enhancement of nanofluids viscosity increases the walls shear stress; therefore the pressure drop of fuel rod bundle will be higher.

Figure 15 shows the heat transfer coefficient of rod bundle for different nanoparticle diameters at $\Phi=1\%$. It can be seen that the heat transfer coefficient increases with decreasing the diameter of nanoparticles. The contact surface between the solid particles and the fluid is enhanced with decreasing the diameter of particles, therefore the heat transfer coefficient raises.

Table 3 shows the total pressure drop of rod bundle nanofluid at volume fraction of 0.01 at different particle diameters and different Reynolds numbers. Results show that by raising the diameter of nanoparticles, the total pressure drop of rod bundle (difference between inlet pressure and outlet pressure) decreases. For example when the diameter of particles increases from 20 to 100 nm, total pressure drop decreases more than 3% at $Re=235000$. Masoumi et al. correlation [21] shows that by increasing the diameter of nanoparticles, the nanofluid viscosity decreases and viscosity reduction of nanofluids yields to lower pressure drop.

6. Conclusion

In this study the flow field and heat transfer characteristics of water- Al_2O_3 nanofluid in VVER-440 fuel rod bundles are numerically investigated. A 60 degree segment of fuel rod bundle consists of 12 fuel rods (8 full rods and 4 half rods), central tube, 4 spacer grids and walls of shroud is considered for simulation. The results can be summarized as follow:
-Addition of Al_2O_3 nanoparticles in base fluid has a significant enhancement in heat transfer compared to that of the pure fluid. Although, the pressure drop for Nanofluids flow is slightly higher than the pressure drop for the pure water flow.

-Increasing nanoparticles volume fraction enhances the heat transfer coefficient. For example, at different Reynolds numbers, by increasing nanoparticles volume fraction from 0.0 to 0.01, the total average of the heat transfer coefficient raises between 28% to 32%.

-By enhancement of nanoparticles volume fraction, total pressure drop rises gradually. For example, at different Reynolds numbers, the increment of nanoparticles volume fraction from 0.0 to 0.05,

yielded to the total pressure drop enhancement between 25% to 29%.

-Decreasing nanoparticles diameter raises pressure drop. For example, at volume fraction of 1%, by decreasing nanoparticles diameter from 100 to 50 nm, the total pressure drop increases between 0.5% to 1% at different Reynolds numbers.

-At different Reynolds numbers, decreasing nanoparticles diameter leads to higher heat transfer coefficient.

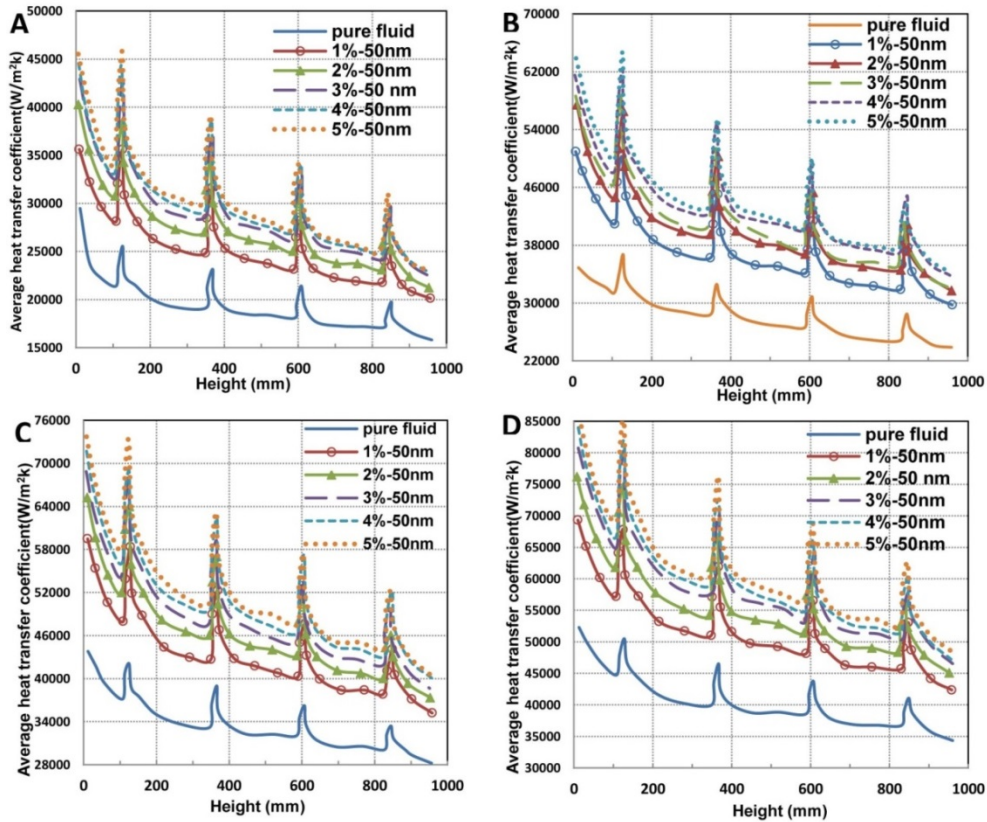


Fig. 13. Heat transfer coefficient at $d_p=50$ nm at different Re: (a) 125000, (b) 203000, (c) 250000, (d) 312000

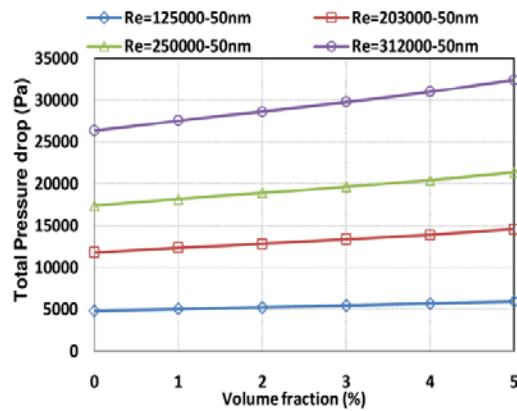


Fig. 14. Total pressure drop in fuel rod bundle ($d_p=50$ nm)

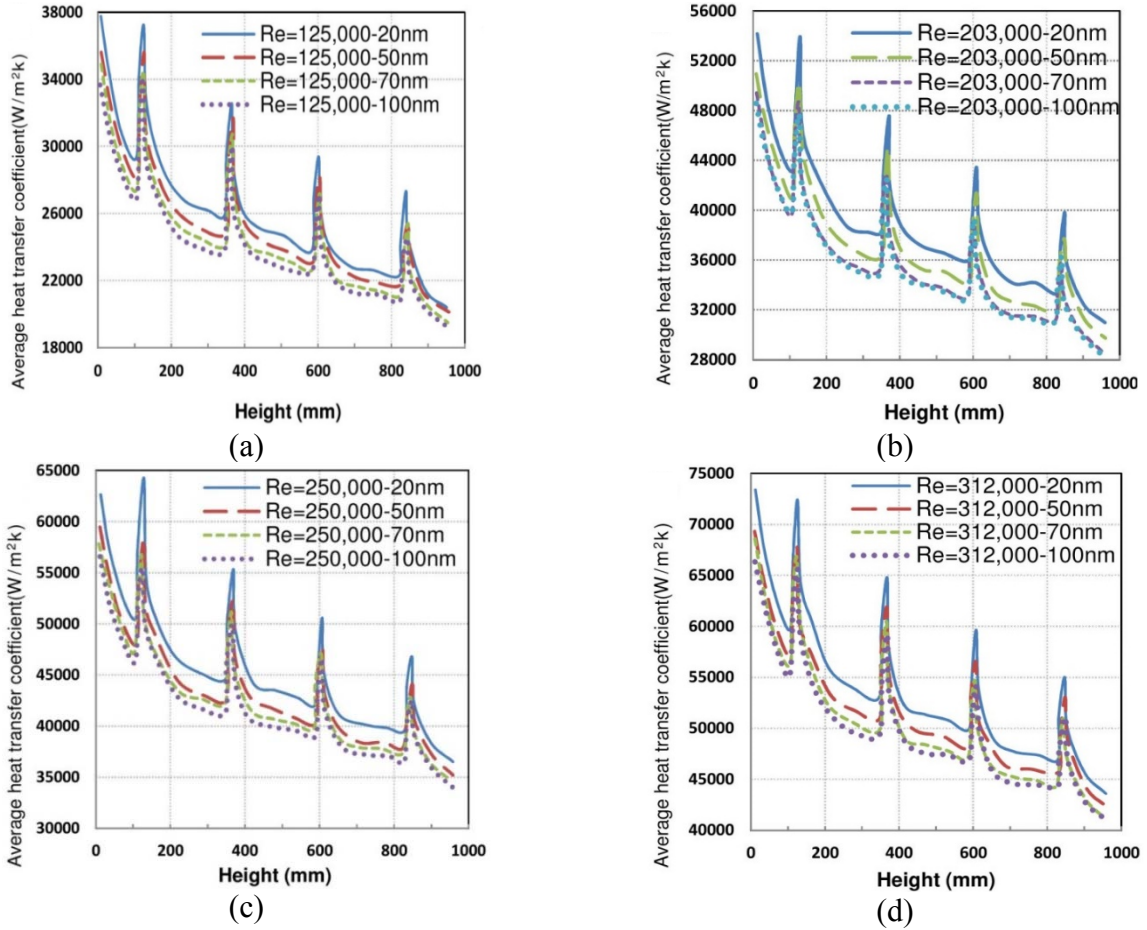


Fig. 15. Heat transfer coefficient at $\phi = 1\%$ at different Re, (a) 125000, (b) 203000, (c) 250000, (d) 312000

Table 2

Mean heat transfer coefficient in rod bundle ($d_p=50$ nm).

Reynolds number	$\phi = 0\%$	$\phi = 1\%$	$\phi = 2\%$	$\phi = 3\%$	$\phi = 4\%$	$\phi = 5\%$
125000	20163	26566	29117	30595	31505	32304
203000	29264	38707	42347	43395	45508	46348
250000	34714	45288	48806	51248	53347	54532
312000	41886	53880	58091	60970	62738	64673

Table 3

Total pressure drop of fuel rod bundle (pa) at $\phi = 1\%$.

Particle diameter	Re= 125000	Re= 203000	Re= 250000	Re= 312000
20 nm	5194	12717	18692	28316
50 nm	5024	12340	18162	27546
70 nm	5004	12297	18102	27457
100 nm	4992	12272	18064	27405

Acknowledgment

The authors gratefully acknowledge the financial support of the Iranian Nanotechnology Initiative Council.

REFERENCES

- [1] M. E. Conner, E. Baglietto, A. M. Elmahdi, CFD methodology and validation for single-phase flow in PWR fuel assemblies, *Nuclear Engineering and Design* 240 (2010) 2088–2095.
- [2] S. Tóth, A. Aszódi, Calculations of coolant flow in a VVER-440 fuel bundle with the code ANSYS CFX 10.0, *Proceedings of the Workshop on Modeling and Measurements of Two-Phase Flows and Heat Transfer in Nuclear Fuel Assemblies*, Stockholm, Sweden (2006).
- [3] M. R. Abdi, M. Asgari, Kh. Rezaee Ebrahim Saraee, M. Talebi, Numerical Simulation of Split Vane in a 60 Fuel Rod Bundle of VVER-440 Reactor and Survey the Effect of Large Length Split Vane (LLSV) and Half-Length Split Vane (HLSV) on Heat Transfer Distribution. *World Applied Sciences Journal* 18 (7) (2012) 909-917.
- [4] B. C. Rahimi, G. Jahanfarnia, Thermal-hydraulic core analysis of the VVER-1000 reactor using a porous media approach, *Journal of Fluids and Structures* 51 (2014) 85–96.
- [5] M. Jabbari, k. Hadad, G. R. Ansarifard, Z. Tabadar, Power calculation of VVER-1000 reactor using a thermal method, applied to primary–secondary circuits, *Annals of Nuclear Energy* 18 (77) (2015) 129-132.
- [6] S.U.S. Choi, Enhancing thermal conductivity of fluid with nanoparticles, *ASME FED* 231/MD. 66 (1995) 99–103.
- [7] P. Keblinski, S. R. Phillpot, S.U.S. Choi, J. A. Eastman, Mechanisms of heat flow in suspensions of nano-sized particles (nanofluid), *Int. J. of Heat and Mass Transfer* 45 (2002) 855–863.
- [8] J. A. Eastman, S. R. Phillpot, S.U.S. Choi, P. Keblinski, Thermal transport in nanofluids, *Annual Review of Materials Research* 34 (2004) 219–246.
- [9] O. Ghaffari, A. Behzadmehr, H. Ajam, Turbulent mixed convection of a nanofluid in a horizontal curved tube using a two-phase approach, *International Communications in Heat and Mass Transfer* 37 (10) (2010) 1551–1558.
- [10] A. Behzadmehr, M. Saffar Avval, N. Galanis, Prediction of turbulent forced convection of a nanofluid in a tube with uniform heat flux using a two phase approach, *Int. J. of Heat and Fluid Flow* 28 (2) (2007) 211–219.
- [11] C. Abdellahoum, A. Mataoui, H. Oztop, Turbulent forced convection of nanofluid over a heated shallow cavity in a duct, *Annals of Nuclear Energy* 277 (2015) 126-134.
- [12] A. Moghadassi, E. Ghomi, F. Parviziyan, A numerical study of water based Al_2O_3 and Al_2O_3 -Cu hybrid nanofluid effect on forced convective heat transfer, *International Journal of Thermal Sciences* 92 (2015) 50–57.
- [13] J. Buongiorno, B. Truong, Preliminary study of water- based nanofluid coolants for PWRs, *Transactions of the American Nuclear Society* 92 (2005) 383–384.
- [14] K. Hadad, A. Hajizadeh, K. Jafarpour, B.D. Ganapol, Neutronic study of nanofluids application to VVER-1000, *Annals of Nuclear Energy* 37(11) (2010) 1447–1455.
- [15] E. Zarifi, G. Jahanfarnia, F. Veysi, Thermal-hydraulic modeling of nanofluids as the coolant in VVER-1000 reactor core by the porous media approach, *Annals of Nuclear Energy* 51 (2013) 203–212.
- [16] K. Hadad, A. Rahimian, M. R. Nematollahi, Numerical study of single and two-phase models of water/ Al_2O_3 nanofluid turbulent forced convection flow in VVER-1000 nuclear reactor, *Annals of Nuclear Energy* 60 (2013) 287-294.
- [17] O. Ltd, User guide, <http://www.openfoam.com/docts/user/>; (2011).
- [18] S. P. Janga, S.U.S. Choi, (Role of Brownian motion in the enhanced thermal conductivity of nanofluids, *Applied Physics Letters* 84 (2004) 4316-4318.
- [19] C. H. Chon, K. D. Kihm, S. P. Lee, S.U.S. Choi, Empirical correlation finding the role of temperature and particle size for nanofluid (Al_2O_3) thermal conductivity enhancement, *Applied Physics Letters* 87 (2005) 153107–153110.
- [20] H. A. Mintsas, G. Roy, C. T. Nguyen, D. Doucet, New Temperature Dependent Thermal Conductivity Data for Water-Based Nanofluids, *Int. J. of Therm. Sci* 48 (2009) 363–371.

- [21] N. Masoumi, N. Sohrabi, A. A. Behzadmehr, New Model for Calculating the Effective Viscosity of Nanofluids, *Journal of Physics D: Applied Physics* 42 (2009) 55501–55506.
- [22] B. C. Pak, Y. I. Cho, Hydrodynamic and HeatTransfer Study of Dispersed Fluids with Submicron Metallic Oxide Particles, *Experimental Heat Transfer* 11 (1998) 151–170.